


 CONSELHO NACIONAL DE DESENVOLVIMENTO CIENTÍFICO E TECNOLÓGICO - CNPq

 CENTRO BRASILEIRO DE PESQUISAS FÍSICAS - CBPF

**NOTAS DE FÍSICA**

CBPF/NF-053/83

DISSIPATION IN HEAVY ION COLLISION

by

C.A. Bertulani and L.C. Gomes

DISSIPATION IN HEAVY ION COLLISION

C.A. Bertulani\* and L.C. Gomes\*\*

\*Departamento de Física Nuclear - I.F. - UFRJ  
Centro de Tecnologia  
Bloco A, 3ª e 4ª andares  
Cidade Universitária - Ilha do Fundão  
21910 - Rio de Janeiro, RJ, Brasil

\*\*Centro Brasileiro de Pesquisas Físicas - CBPF  
Rua Dr. Xavier Sigaud, 150  
22290 - Rio de Janeiro, RJ - Brasil

## RESUMO

Estuda-se o estágio inicial da evolução de duas esferas de Fermi não superpostas fazendo uso da equação cinética de Uehling-Uhlenbeck. Mostra-se que o tempo de relaxação para a energia relativa (até 50 MeV por nucleon) é dado em termos de uma função dependente somente de dois parâmetros adimensionais. Fazendo uso da aproximação de densidade local aplica-se este resultado às reações altamente inelásticas de íons pesados.

## ABSTRACT

The initial stage of the evolution of two non-overlapping Fermi spheres is studied using the Uehling-Uhlenbeck kinetic equation. The relaxation time for the relative energy, up to 50 MeV per nucleon, is shown to be given by a function dependent only on two dimensionless parameters. Making use of the local density approximation this result has been applied to deep inelastic collisions.

## 1. INTRODUCTION

The analysis of heavy ion collisions have exhibited a spectacular transfer of energy from the relative motion of the ions to internal degrees of freedom of the emergent fragments <sup>(1)</sup>, referred as deep inelastic collisions. In the transfer process there seems to be involved two major mechanisms: (i) The immediate dissipation of energy and (ii) the coherent vibrations of the two fragments. The latter mechanism is best seen in the TDHF simulations of such collisions <sup>(2)</sup>. Though the single particle motions are fully taken under consideration in this approximation, the lack of two-particle collisions precludes any sort of energy dissipation. In this paper we will discuss the dissipation mechanism on the basis of the Uehling-Uhlenbeck kinetic equation and the local density approximation for collisions up to 50 MeV per nucleon. The approximations involved are of such a nature as to guarantee that our calculation, apart from the local density approximation, is an upper limit to the contribution of dissipation in heavy ion collisions. Similar calculations have been reported by Albrecht and Stocker <sup>(3)</sup> and Toepffer and Wong <sup>(4)</sup>. In ref. <sup>(3)</sup> the exclusion principle is not fully taken under consideration and the calculation is adapted to low energy per nucleon. In our case we have fully taken under consideration the exclusion principle and we interpret the initial state of local system as two non-overlapping Fermi spheres. In ref. <sup>(4)</sup> the calculation is very similar to ours except for the initial local state is taken as two Fermi spheres with their centers only slightly displaced one with respect to the other.

In section 2 we state our basic model and show in section

3 how we calculate relaxation times. In section 4 we make a comparison with the phenomenological viscous force in deep inelastic scattering and in section 5 we state our major conclusions.

## 2. THE BASIC MODEL

We consider two nuclear matters moving one against the other with relative velocity  $\vec{v}_0$ ,

$$\vec{v}_0 = \frac{h}{m} \vec{k}_0 \quad , \quad (2.1)$$

where  $m$  in the above equation is the nucleon mass. The nuclear matters may have different densities characterized by their Fermi momenta but we will assume equal number of protons and neutrons in both of them. We therefore observe that the initial state of the system is described in momentum space by two filled spheres of radii  $k_{F>}$  and  $k_{F<}$ , corresponding respectively to the larger and smaller spheres, with the position of the center of the smaller sphere with respect to the center of the larger one given by  $\vec{k}_0$ . The exclusion principle requires that

$$k_0 \geq k_{F>} + k_{F<} \quad .$$

Our purpose in this section will be to describe the initial evolution of this state by using the Uehling-Uhlenbeck equation. Due to our assumption of equal number of protons and neutrons and the charge independence of the nuclear force each one of the four kind of nucleons (neutrons or protons with spins up or

down) has at all times the same distribution in momentum space. We will therefore ignore in what follows the internal degrees of freedom of the nucleons. The Uehling-Uhlenbeck equation can be written as

$$\frac{\partial n(\vec{k}_1)}{\partial t} = G(\vec{k}_1) - L(\vec{k}_1) \quad (2.3)$$

where the gain and loss terms are respectively:

$$G = \frac{\hbar}{m} (1-n_1) \int \frac{d^3k_2}{(2\pi)^3} |\vec{k}_2 - \vec{k}_1| (1-n_2) \int d\Omega n'_1 n'_2 \frac{d\sigma}{d\Omega} \quad , \quad (2.4)$$

and

$$L = \frac{\hbar}{m} n_1 \int \frac{d^3k_2}{(2\pi)^3} |\vec{k}_2 - \vec{k}_1| n_2 \int d\Omega (1-n'_1) (1-n'_2) \frac{d\sigma}{d\Omega} \quad . \quad (2.5)$$

The function  $n(\vec{k})$  is the occupation number for momentum state  $\vec{k}$  and we have used in the above equations the short notation:

$$n'_1 = n(\vec{k}'_1) \quad , \quad \text{etc...}$$

The four momenta  $\vec{k}_1$ ,  $\vec{k}_2$ ,  $\vec{k}'_1$  and  $\vec{k}'_2$  are related by the conservation laws:

$$\vec{k}_1 + \vec{k}_2 = \vec{k}'_1 + \vec{k}'_2$$

$$\vec{k}'_1 - \vec{k}'_2 = \vec{\epsilon} |\vec{k}_1 - \vec{k}_2|$$

where  $\vec{\epsilon}$  is a unit vector in the direction of the solid angle  $d\Omega$  and  $\frac{d\sigma}{d\Omega}$  is the differential cross-section of a pair of nucleons. It is interesting to observe that if  $n(\vec{k}) \ll 1$  everywhere in momentum space then the Uehling-Uhlenbeck equation goes over to

the well-known Boltzmann equation. In a loose sense the Uehling-Uhlenbeck equation is the Boltzmann equation corrected for the exclusion principle.

At the initial stage of evolution,  $L$  is different from zero only inside both spheres due to the presence of the factor  $n(\vec{k}_1)$  in eq. (2.5). On the other hand  $G$  is different from zero only outside both spheres because the presence of the factor  $[1-n(\vec{k}_1)]$  in eq. (2.4). Besides, collision of nucleons in the same sphere is forbidden because the exclusion principle. Therefore, the collision mechanism depletes both spheres simultaneously throwing the colliding pair of nucleons into the outside region.

For  $\frac{d\sigma}{d\Omega}$  we have made the following approximations: We have assumed that

$$\sigma_{nn} = \sigma_{pp} = \frac{1}{4} \sigma_{np}$$

and we have also neglected the angular dependence of  $\frac{d\sigma}{d\Omega}$ . Therefore, taking  $\sigma_{np}$  for the total cross-section for neutron-proton scattering we have set<sup>(\*)</sup>

$$\frac{d\sigma}{d\Omega} = \frac{5}{2} \left( \frac{\sigma_{np}}{4\pi} \right) \quad (2.6)$$

For  $\sigma_{np}$  we have assumed the following dependence with the energy:

$$\sigma_{np} = \frac{\sigma_0}{|k_1 - k_2|^2} \quad (2.7)$$

where  $\sigma_0$  is a dimensionless constant. In Fig. 1 it is plotted  $\log \sigma_{np}$  as a function of the logarithm of the energy of the pair

---

(\*) The factor  $5/2$  comes from the average cross-section  $(5/8 \sigma_{np})$  and the fact that we are dealing with four kind of particles.

in the laboratory frame of reference. The points are experimental data <sup>(5)</sup> and the straight line corresponds to the assumption given by eq. (2.7) with  $\sigma_0 = 39.4$ . One may observe that the law given by eq. (2.7) describes reasonably well the data except towards the low energy limit where eq. (2.7) overestimates the experimental value of  $c_{np}$ .

The integration over the solid angles in eqs. (2.4) and (2.5) can be done exactly and it is shown in the appendix. Let us introduce dimensionless variables

$$\begin{aligned} \vec{x} &= \vec{k}_1/k_{F>} , \\ \vec{y} &= \vec{k}_2/k_{F>} , \\ \eta &= k_{F'}/k_{F>} \\ \lambda &= k_0/k_{F>} . \end{aligned} \tag{2.8}$$

and

We have

$$\omega_L(\vec{x}, \vec{y}, \eta, \lambda) = \frac{1}{4\pi} \int d\Omega (1-n_1') (1-n_2') \tag{2.9}$$

and

$$\omega_G(\vec{x}, \vec{y}, \eta, \lambda) = \frac{1}{4\pi} \int d\Omega n_1' n_2' \tag{2.10}$$

where  $\omega_L$  and  $\omega_G$  are weighting factors for the loss and gain terms respectively that tell us the fraction of the solid angle permissible for collision of a pair of nucleons.

The loss and gain terms take the form

$$L(\vec{x}, \eta, \lambda) = 5\sigma_0 \frac{E_{F>}}{\hbar} n(\vec{x}) \int \frac{d^3y}{(2\pi)^3} \frac{n(\vec{y})}{|\vec{x}-\vec{y}|} \omega_L(\vec{x}, \vec{y}, \eta, \lambda) \tag{2.11}$$

and



$$G(\vec{x}, \eta, \lambda) = 5\sigma_0 \frac{E_{F>}}{\hbar} [1-n(\vec{x})] \int \frac{d^3y}{(2\pi)^3} \frac{[1-n(\vec{y})]}{|\vec{x}-\vec{y}|} \omega_G(\vec{x}, \vec{y}, \eta, \lambda) \quad (2.12)$$

where

$$E_{F>} = \frac{\hbar^2 k_{F>}^2}{2m}$$

is the Fermi energy associated to the larger sphere.

The three dimensional integrations in eqs. (2.11) and (2.12) were done by Monte Carlo method. In Fig. 2 we exhibit a typical result for  $L(\vec{x}, \eta, \lambda)$ . We have taken  $\lambda = 2$  and  $\eta = 0.5$ . The function  $L$  has cylindrical symmetry in  $x$ -space and we plotted in Fig. 2 curves of constant values of  $L$ . The values of  $L$  indicated along the constant lines are normalized such that its integral inside one of the spheres is equal to unit. We have also drawn the contour of the two spheres. One observes that two mechanisms compete to produce the pattern exhibited in Fig. 2: The exclusion principle favours the depletion of the large momentum particles and the energy dependence of the cross-section favours the small momentum collisions. This results in the appearance, in the large sphere, of a region of least probability of collision somewhere near its equatorial plane. In Fig. 3 we exhibit plots of constant values for  $G$ , again for  $\lambda = 2$  and  $\eta = 0.5$ . The values of  $G$  indicated along the constant lines have the same normalization used for  $L$  in Fig. 2. Here it is interesting to observe that the collisions favor the insertion of particles in a toroidal region near the plane passing in between the two spheres.

### 3. THE RELAXATION TIME

Let us refer all momenta to the center of mass system of the two nuclear matters. In momentum space the two filled spheres considered in the previous section have their centers given by

$$\vec{k}_{<} = \frac{\rho_{>}}{\rho_{<} + \rho_{>}} \vec{k}_0$$

and

$$\vec{k}_{>} = - \frac{\rho_{<}}{\rho_{<} + \rho_{>}} \vec{k}_0$$

where  $\rho_{<}$  and  $\rho_{>}$  are the smaller and larger densities of particles of the two nuclear matters respectively. The relative energy per particle of the two nuclear matters  $E(t)$  may be defined as

$$E(t) = \frac{\hbar^2}{m(\rho_{<} + \rho_{>})} \int [3 \frac{(\vec{k} \cdot \vec{k}_0)^2}{k_0^2} - k^2] n(\vec{k}, t) \frac{d^3 k}{(2\pi)^3} .$$

At the initial state of the system we have

$$E(0) = \frac{1}{2} \left[ \frac{\rho_{<} \rho_{>}}{(\rho_{<} + \rho_{>})^2} \right] \frac{\hbar^2 k_0^2}{m}$$

which is the usual expression for the relative energy per particle of the two nuclear matters. As the systems evolves, the distribution of particles approaches a spherically symmetrical distribution and  $E(t)$  approaches zero. We therefore take the quantity  $\zeta$  defined as

$$-\zeta(t) = \frac{dE/dt}{E}$$

as a measure of the rate at which the relative energy of the motion is dissipated. Its reciprocal value we take as the relaxation time

for the relative motion of the two nuclear matters. At the initial stage of evolution we have

$$\zeta(0) = \frac{\hbar^2}{m(\rho_{<} + \rho_{>})E(0)} \int [3 \frac{(\vec{k} \cdot \vec{k}_0)^2}{k_0^2} - x^2] \frac{\partial n(\vec{k}, 0)}{\partial t} \frac{d^3 k}{(2\pi)^3}$$

We will set

$$\zeta = \frac{2E_{F>}}{\hbar} \phi(\eta, \lambda) \quad (3.1)$$

where, making use of eqs. (2.11), (2.12) and (2.3) we obtain

$$\begin{aligned} \phi(\eta, \lambda) = & 5\sigma_0 \frac{(1+\eta^3)}{\eta^3} \frac{1}{\lambda^2} \int \frac{d^3 x}{(2\pi)^3} [3 \frac{(\vec{x} \cdot \vec{k}_0)^2}{k_0^2} - x^2] \\ & \times \{ [1 - n(\vec{x})] \int \frac{d^3 y}{(2\pi)^3} \frac{[1 - n(\vec{y})]}{|\vec{x} - \vec{y}|} \omega_G(\vec{x}, \vec{y}, \eta, \lambda) \\ & - n(\vec{x}) \int \frac{d^3 y}{(2\pi)^3} \frac{n(\vec{y})}{|\vec{x} - \vec{y}|} \omega_L(\vec{x}, \vec{y}, \eta, \lambda) \} \end{aligned} \quad (3.2)$$

Due to the cylindrical symmetry of the problem this integration reduces to a five dimensional one which we have done by Monte Carlo method within a 10% statistical error. They were further smoothed out by spline adjustments. It is the smoothed data that are plotted in Figs. 4, 5 and 6. Fig. 4 exhibits  $\phi(\eta, \lambda)$  as a function of  $\eta$  for values of  $\lambda$  between 1.2 to 2.0. We observe that the domains of  $\eta$  in this range are restricted to

$$0 \leq \eta \leq \lambda - 1$$

Fig. 5 exhibits  $\phi(\eta, \lambda)$  again as a function of  $\eta$  for values of  $\lambda$  from 2.0 to 8.0. Finally, Fig. 6 shows  $\phi(\eta, \lambda)$  as a function of  $\lambda$

for  $\eta = 1.0$ . We would like to stress that the calculation of the basic quantity  $\zeta$ , which characterizes the time scale for the evolution of the two nuclear matters, is reduced to the determination of  $\phi(\eta, \lambda)$ . As an example two nuclear matters of equal densities ( $\eta = 1.0$ ) with relative velocity such as  $\lambda = 2.0$  and  $k_F = 1.35 \text{ Fm}^{-1}$  have a relaxation time  $\tau$  given by

$$\tau = \frac{1}{\zeta} = \frac{\hbar}{2E_F} \phi^{-1}(1., 2.) = 1.6 \times 10^{-22} \text{ s} .$$

#### 4. APPLICATION TO DEEP INELASTIC COLLISIONS

In order to apply the results of our calculation to deep inelastic collisions we will consider the particular case of  $\text{Ar}_{18}^{40}$  with  $\text{Th}_{90}^{232}$  at 379 MeV incident energy in the laboratory frame of reference. Barbosa (\*) has studied this reaction by using a model similar to the one used by Gross and Kalinowski (6). For the nuclear interaction he used the proximity potential of Randrup et al. (7) and the viscosity had a gaussian form factor that reproduced the Gross-Kalinowski results in the deep inelastic region. In both models the viscosity is the only mechanism responsible for the loss of the relative energy of the ions during the collision. One can easily prove that

$$\frac{dE}{dt} = - \frac{1}{2} \zeta_{ij} v_i v_j$$

along any orbit where  $\zeta_{ij}$  is the viscosity tensor (\*\*\*) and  $v_i$  are

---

(\*) We would like to thank Valmar Barbosa for having kindly help us with this calculation.

(\*\*) Both authors use different viscosity for the tangencial and radial relative motion of the ions.

the components of the relative velocity of the ions. Let us define

$$\bar{\zeta} = \frac{\zeta_{ij} v_i v_j}{v^2}$$

as the mean viscosity. We have

$$\int_{E_i}^{E_f} \frac{dE}{E} = - \int_{-\infty}^{\infty} dt \bar{\zeta} .$$

Therefore,

$$\text{Log} \left( \frac{E_f}{E_i} \right) = - \int_{-\infty}^{\infty} dt \bar{\zeta}$$

where  $E_f$  and  $E_i$  are the final and the initial relative energy of the ions respectively. For the particular reaction under consideration the critical value for the angular momentum was found to be  $124\hbar$ . Taking an orbit initiated with angular momentum equal to  $128\hbar$ , we found  $E_f = 228$  MeV and as  $E_i = 323$  MeV we obtained

$$\int \bar{\zeta} dt = 0.34 . \quad (4.1)$$

To apply our basic model to the estimation of the two body viscosity in deep inelastic collisions we have taken the same orbit as above, i.e., the same values of relative position and relative velocity as function of time. We have assumed that the ions react with their density frozen which we have taken to be the Woods-Saxon form factor with the usual parameters <sup>(8)</sup>. At every instant of time we have

$$-\frac{dE(t)/dt}{E} = \frac{1}{A} \int \rho(\vec{r}, \vec{R}) \zeta(\vec{r}, \vec{R}, \vec{v}) d^3 r \equiv \zeta(t) \quad (4.2)$$

where the auxiliary coordinate  $\vec{r}$  gives the position of a point in the particle distribution of the ions at a given relative position  $\vec{R}$  of their centers of mass.  $\zeta(\vec{r}, \vec{R}, \vec{v})$  is taken as given by eq.

(3.1) where  $k_{F<}(\vec{r}, \vec{R})$  and  $k_{F>}(\vec{r}, \vec{R})$  are given by the local density approximation and

$$k_0 = \frac{mv}{\hbar} .$$

In eq. (4.2)  $\rho(\vec{r}, \vec{R})$  is the sum of the densities of the two ions. From eq. (4.2) we have obtained

$$\int \zeta(t) dt = 0.020 . \quad (4.3)$$

Comparing the results of eqs. (4.1) and (4.3) we conclude that the two-body viscosity is on average 17 times smaller than the phenomenological viscosity used in models similar to Gross and Kalinowski.

## 5. CONCLUSIONS

We have introduced a basic model for the understanding of dissipation in heavy ion collisions. As we have in mind the local density approximation our basic model consists of two nuclear matters of different densities moving one against the other with a given relative velocity<sup>(\*)</sup>. We have studied the evolution of such a state by using the Uehling-Uhlenbeck equation. Assuming isotropic two-body cross section inversely proportional to the

---

<sup>(\*)</sup>We have not considered different densities for protons and neutrons.

energy, we were able to calculate the logarithm rate of change of the relative kinetic energy of the two nuclear matters at the initial stage of evolution. This rate of change was shown to be given by a function dependent only on two dimensionless parameters:  $\eta$  being the ratio of the smaller to the larger Fermi momenta and  $\lambda$  being the ratio of the relative momentum per nucleon to the larger Fermi momentum. Once this function is tabulated the dissipation of relative energy in heavy-ion collision can easily be calculated in the local density approximation at different kinematical conditions.

To have an idea of how large the dissipation is we estimated it for two nuclear matters of equal density ( $k_F = 1.35 \text{ Fm}^{-1}$ ) with relative energy corresponding to 38 MeV per nucleon. The relaxation time for this system comes to be approximately equal to the time that one heavy ion passes through the other ( $2 \times 10^{-22} \text{ s}$ ).

We would like to mention that the approximations involved in our calculation are all biased to underestimate the relaxation times. We will point out four of them:

- 1 - The use of an inverse energy law for the two-nucleon cross section overestimates the experimental cross section in the low energy limit and therefore contributes to underestimate the relaxation times;
- 2 - Similar effect is also due to the assumption of isotropic cross section as the experimental cross-sections, towards the high energy region of interest, is actually lower at the  $90^\circ$  angle in the center of mass reference frame of the pair and it is this angular region that contributes most to the dissipation mechanisms;
- 3 - The Uehling-Uhlenbeck equation neglects the exclusion principle

in the intermediate states of the colliding pair what contributes to lowering the actual two-nucleon cross section in nuclear matter and thus having also the effect of underestimating the relaxation time;

- 4.- By calculating the relaxation time at the initial state of evolution we have also underestimated it as we are, in this situation, emphasizing the fast modes of decay of the distribution in detriment to the slow ones.

These reasonings suggest therefore that, in application to heavy-ion collisions, our basic model overestimates the viscous force. It is important to observe that our calculation has no adjustable parameters and takes into full account the exclusion principle in the final states.

Applying our results to the deep inelastic collision of  $^{40}_{18}\text{Ar} + ^{232}_{90}\text{Th}$  ( $E_{\text{lab}} = 379 \text{ MeV}$ ) we were able to show that on average, along a typical trajectory, the energy dissipation predicted by our model was 17 times smaller than the one predicted by the Gross-Kalinowski model. As their model uses practically only radial friction (the tangential coefficient of viscosity is 400 times smaller than the radial one) we conclude that the viscous force predicted by our model is 12 times larger than its tangential viscous force but 34 times smaller than its radial one. This points to the fact that the two-body viscosity is the major mechanism for dissipation of angular momentum in deep inelastic collisions. On the other hand the very large value of the radial viscosity of Gross and Kalinowski model suggests, as has been already pointed out <sup>(9)</sup>, the intermediation of the coherent excitations of nuclear vibrations in deep inelastic collisions.



## APPENDIX A

### CALCULUS OF $\omega_L$ AND $\omega_G$

Let us consider two particles, one in each sphere with momenta  $\vec{k}_1$  and  $\vec{k}_2$ . We define

$$\begin{aligned}\vec{p} &= \frac{\vec{k}_1 + \vec{k}_2}{2} \\ \vec{q} &= \frac{\vec{k}_2 - \vec{k}_1}{2}\end{aligned}\tag{A.1}$$

and

$$\vec{b} = \vec{k}_0 - \vec{p}$$

After the collision  $\vec{p}$  and  $\vec{b}$  stay constant while  $\vec{q}$  changes only in direction.

Fig. A.1 exhibits schematically the geometry of the collision. The allowed scattering angle corresponds to the non-shaded region of the sphere with center at  $\vec{p}$  and radius equal to  $q$ .

The admissible angles for the initial pairs to be able to scatter corresponds to the cross-hatched region in Fig. A.1. We call  $\bar{\Omega}$  the solid angle corresponding to this region. We have

$$4\pi\omega_L = 4\pi - (\Omega_a + \Omega_b - \bar{\Omega})$$

and

$$4\pi\omega_G = \bar{\Omega}$$

where

$$\Omega_a = 4\pi (1 - \cos\theta_a) ,$$

$$\Omega_b = 4\pi (1 - \cos\theta_b) .$$

The angles  $\theta_a$  and  $\theta_b$  can easily be related to the momenta defined in eqs. (A.1) and we have obtained

$$\cos\theta_a = \frac{p^2 + q^2 - k_{F<}^2}{2pq}$$

and

$$\cos\theta_b = \frac{b^2 + q^2 - k_{F>}^2}{2bq} .$$

For the calculation of  $\bar{\Omega}$  let us introduce the angle  $\theta$  between the two constant vectors  $\vec{b}$  and  $\vec{p}$ . We have to consider the following cases ( $\theta_a + \theta_b + \theta \leq \pi$ ):

i) if  $\theta \leq \theta_a - \theta_b \leq 0$  we have

$$\bar{\Omega} = \Omega_b ;$$

ii) if  $\theta \leq \theta_b - \theta_a \leq 0$  we have

$$\bar{\Omega} = \Omega_a ;$$

iii) if  $\theta \geq \theta_a + \theta_b$  then

$$\bar{\Omega} = 0 ;$$

iv) if  $|\theta_a - \theta_b| \leq \theta \leq \theta_a + \theta_b$  we have found after some tedious calculation

$$\bar{\Omega} = 4\Omega'(\theta, \theta_a, \theta_b)$$

where

$$\begin{aligned}
 \Omega'(\theta, \theta_a, \theta_b) = & -\cos\theta_a \operatorname{arc\,cos} \left[ \frac{\cos\theta_b - \cos\theta\cos\theta_a}{\operatorname{sen}\theta\operatorname{sen}\theta_a} \right] \\
 & - \cos\theta_b \operatorname{arc\,cos} \left[ \frac{\cos\theta_a - \cos\theta\cos\theta_b}{\operatorname{sen}\theta\operatorname{sen}\theta_b} \right] \\
 & + \operatorname{arc\,cos} \left[ \frac{\cos\theta_b - \cos\theta\cos\theta_a}{\operatorname{sen}\theta_a \sqrt{\cos^2\theta_a + \cos^2\theta_b - 2\cos\theta\cos\theta_a\cos\theta_b}} \right] \\
 & + \operatorname{arc\,cos} \left[ \frac{\cos\theta_a - \cos\theta\cos\theta_b}{\operatorname{sen}\theta_b \sqrt{\cos^2\theta_a + \cos^2\theta_b - 2\cos\theta\cos\theta_a\cos\theta_b}} \right] .
 \end{aligned}$$

In the case where  $\theta_a + \theta_b + \theta > \pi$  we must have

$$\bar{\Omega} = 4 [\Omega'(\theta, \theta_a, \theta_b) + \Omega'(\pi - \theta, \theta_a, \theta_b)] .$$

FIGURE CAPTIONS

FIG. 1 - Experimental data and adjusted curve for the total neutron-proton cross section. The horizontal scale indicates in a logarithm scale the energy of the pair in laboratory frame of reference. The vertical scale indicates in a logarithm scale the total neutron-proton cross section in milibarns. The straight line is a plot of eq. (2.7) with  $\sigma_0 = 39.4$ . The points are experimental data <sup>(5)</sup>.

FIG. 2 - The function  $L(\vec{x}, \eta, \lambda)$  normalized to unit in each Fermi sphere for  $\lambda = 2.0$  and  $\eta = 0.5$ . Apart from the two circles that indicate the contour of the two Fermi spheres the curves exhibited are lines of constant value for  $L$  with the corresponding value indicated over the line.

FIG. 3 - The same as Fig. 2 for  $G(\vec{x}, \eta, \lambda)$ .

FIG. 4 - The function  $\phi(\eta, \lambda)$  as defined by equation (3.1). The curves exhibit  $\phi$  for the values of  $\lambda$  as indicated. The horizontal scale indicates the dimensionless parameter  $\eta$ . The vertical scale indicates one thousand times the values of  $\phi$ .

FIG. 5 - The same as Fig. 4 for values of  $\lambda$  from 2.0 to 8.0 as indicated.

FIG. 6 - The function  $\phi(\eta, \lambda)$  as a function of  $\lambda$  for  $\eta = 1.0$ . The vertical scale is the same as in Fig. 4. The horizontal scale indicates the values of  $\lambda$ .

FIG.A.1 - Diagram exhibiting the kinematics of the two nucleon collision. The two Fermi spheres are indicated by  $F_<$  and  $F_>$ . The initial momenta of the pair,  $\vec{k}_1$  and  $\vec{k}_2$ , together with  $\vec{k}_0$ ,  $\vec{p}$  and  $\vec{q}$  are represented by arrows as indicated. The third sphere is the loci of the end points of the vector  $\vec{q}'$ . The non-shaded region corresponds to the allowed scattering

angle. The cross-hatched region indicates the admissible angles for initial pairs with the same total momentum  $2\vec{p}$  and the same modulus  $q$  for the relative momentum.

REFERENCES

- (1) - A.G. Artukh, G.F. Gridnev, V.L. Mikheev, V.V. Volkov and J. Wilczynski, Nucl. Phys. 215 (1973) 91.
- (2) - K.T.R. Davies and S.E. Koonin, Phys. Rev. C23, 2042 (1981)  
A.K. Dhar in Nuclear Physics, C.H. Dasso, R.A. Broglia and A. Winther (eds.), North-Holland Publishing Company, 1982.
- (3) - K. Albrecht and W. Stocker, Nucl. Phys. A278(1977)95.
- (4) - C. Toepffer and C.Y. Wong, Phys. Rev. C 25, 1018 (1982).
- (5) - Landolt-Börnstein, Vol. I-9 (Springer, Heidelberg, 1980).
- (6) - D.H.E. Gross and H. Kalinowski, Phys. Rep. 45 (1978) 175.
- (7) - J. Blocki, J. Randrup, W.J. Swiatecki and C.F. Tsang, Ann. Phys. 105 (1977) 427.
- (8) - Landolt-Börnstein, Vol. I-2 (Springer, Heidelberg, 1980).
- (9) - R.A. Broglia, C.H. Dasso and A. Winther, in Proceedings of the International School of Physics E. Fermi, Course LXXVII, Edited by R.A. Broglia, C.H. Dasso and R. Ricci, North Holland, Amsterdam, 1981.

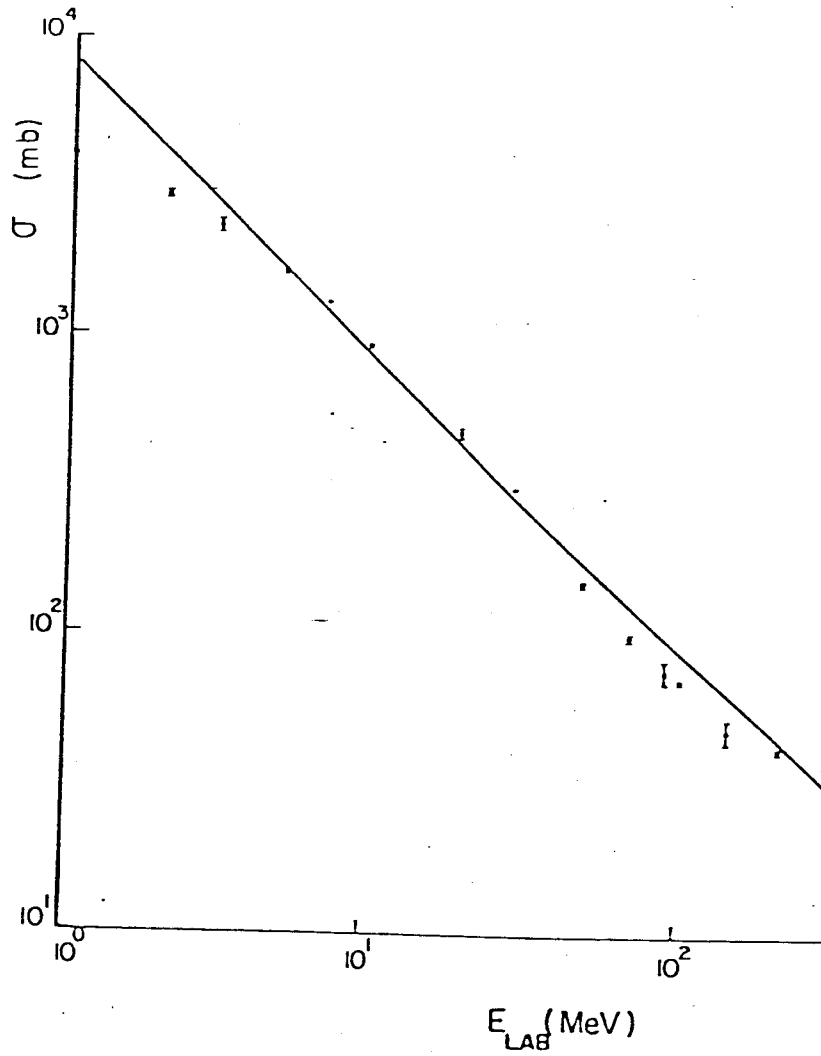


FIGURE 1

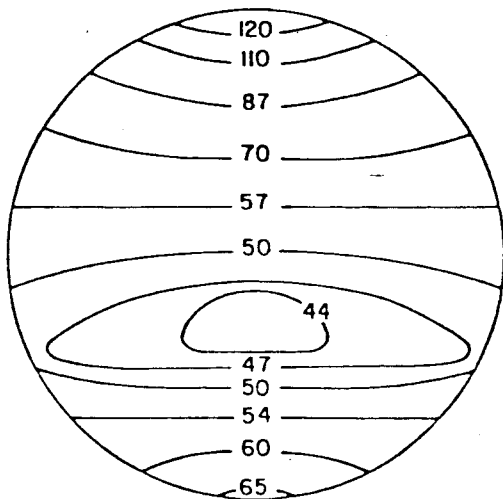
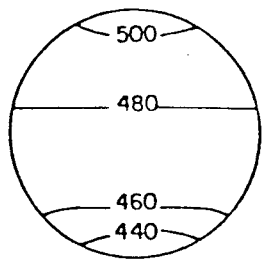


FIGURE 2



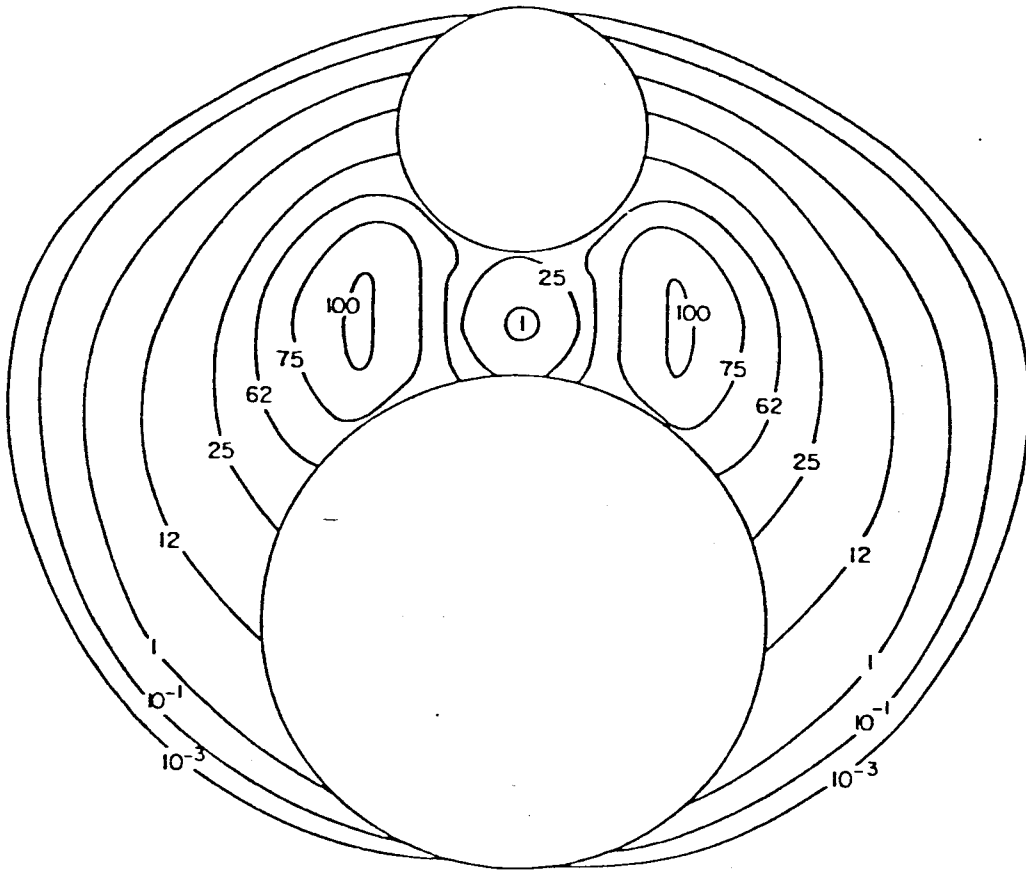


FIGURE 3

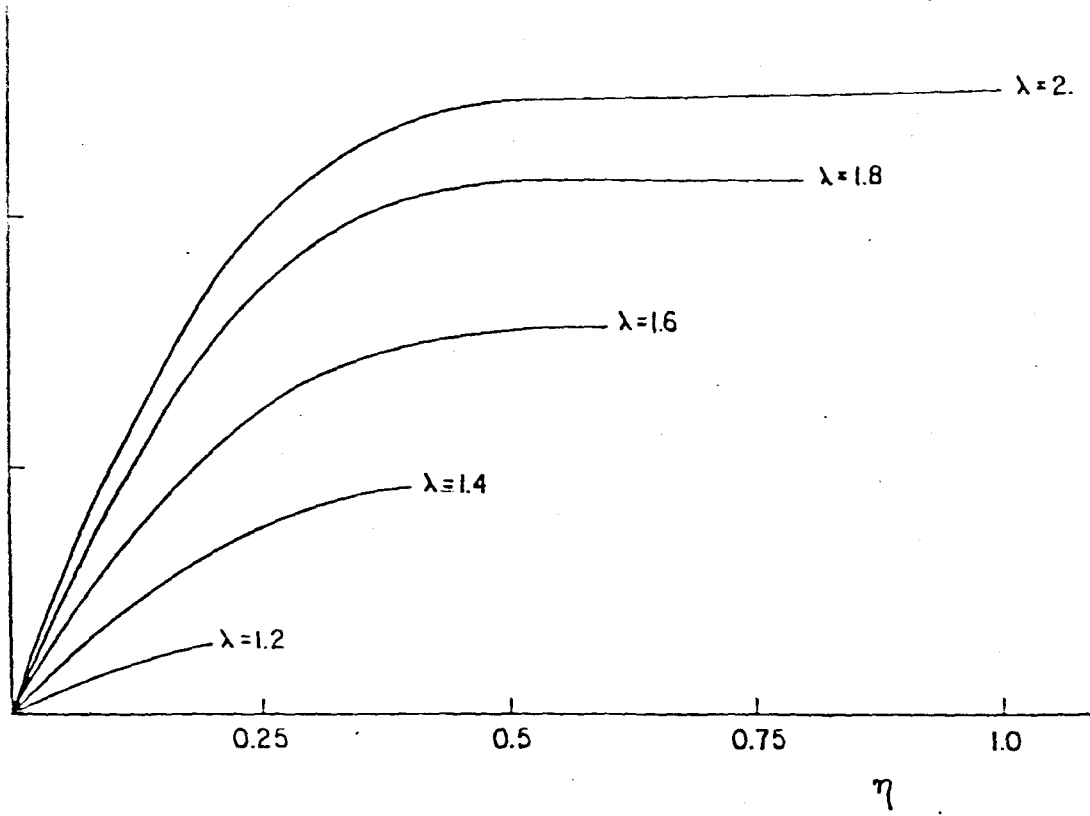


FIGURE 4

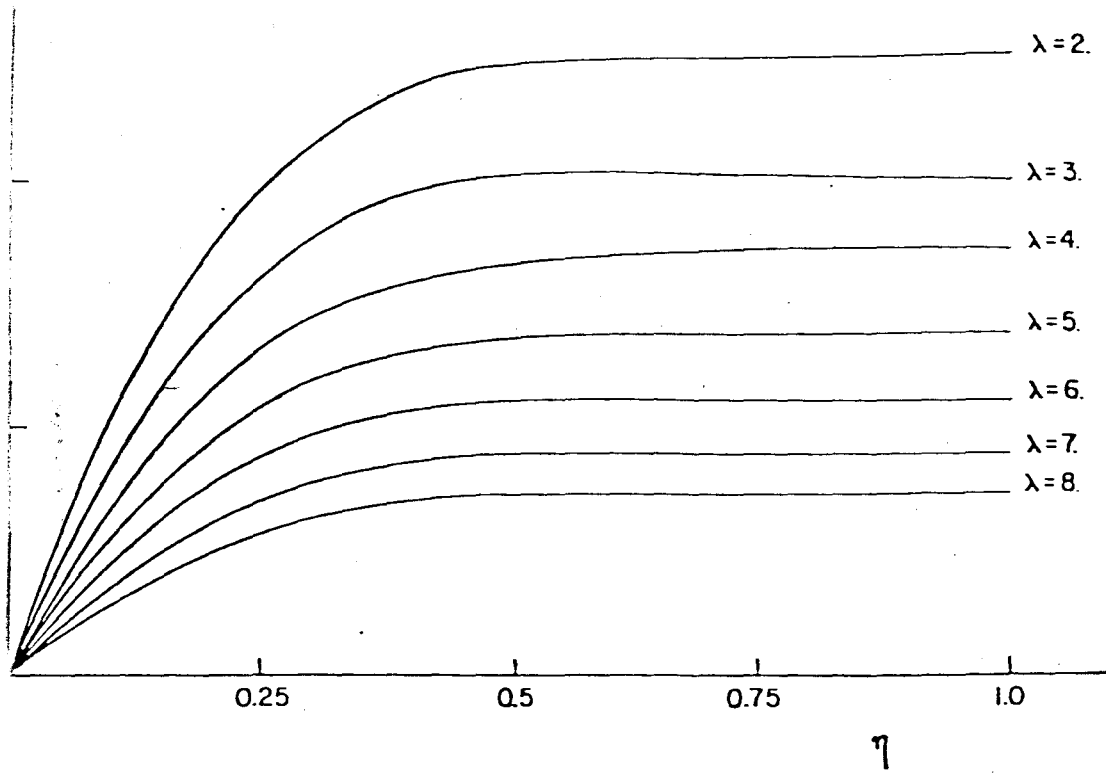


FIGURE 5

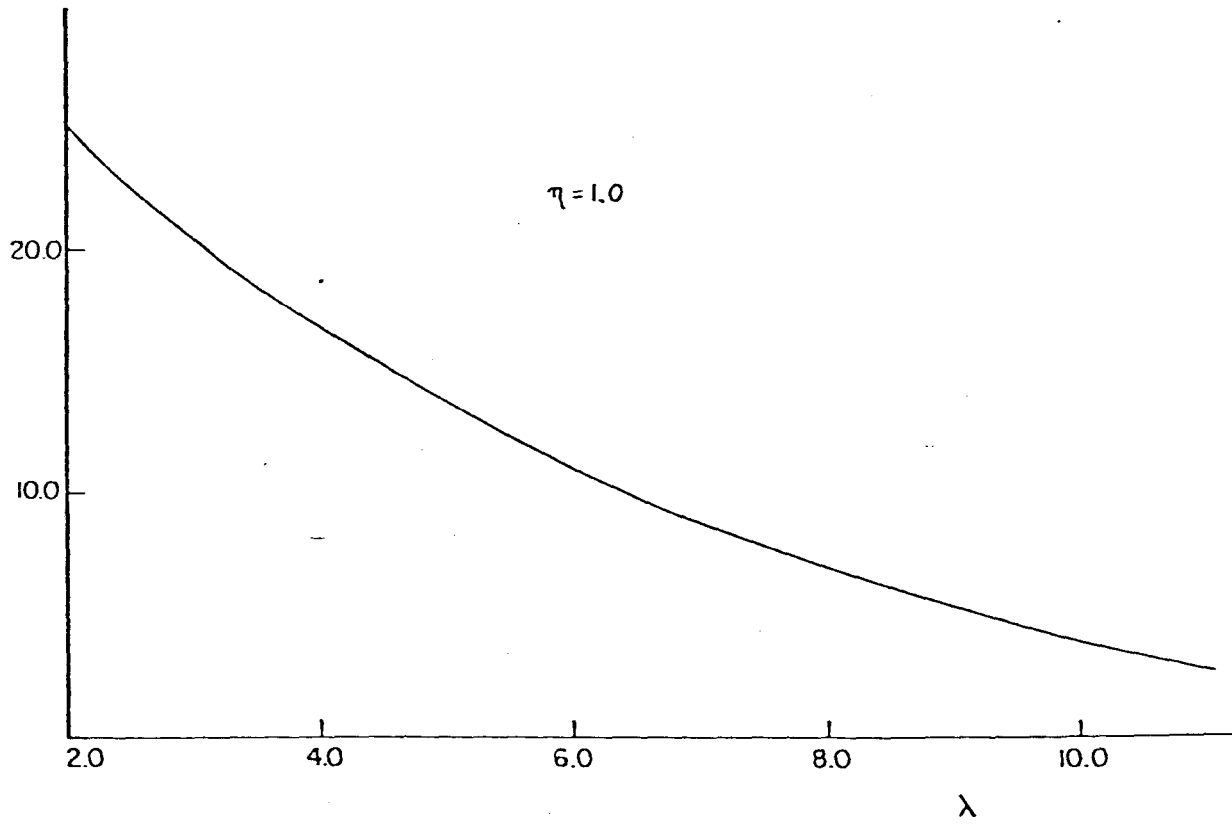


FIGURE 6

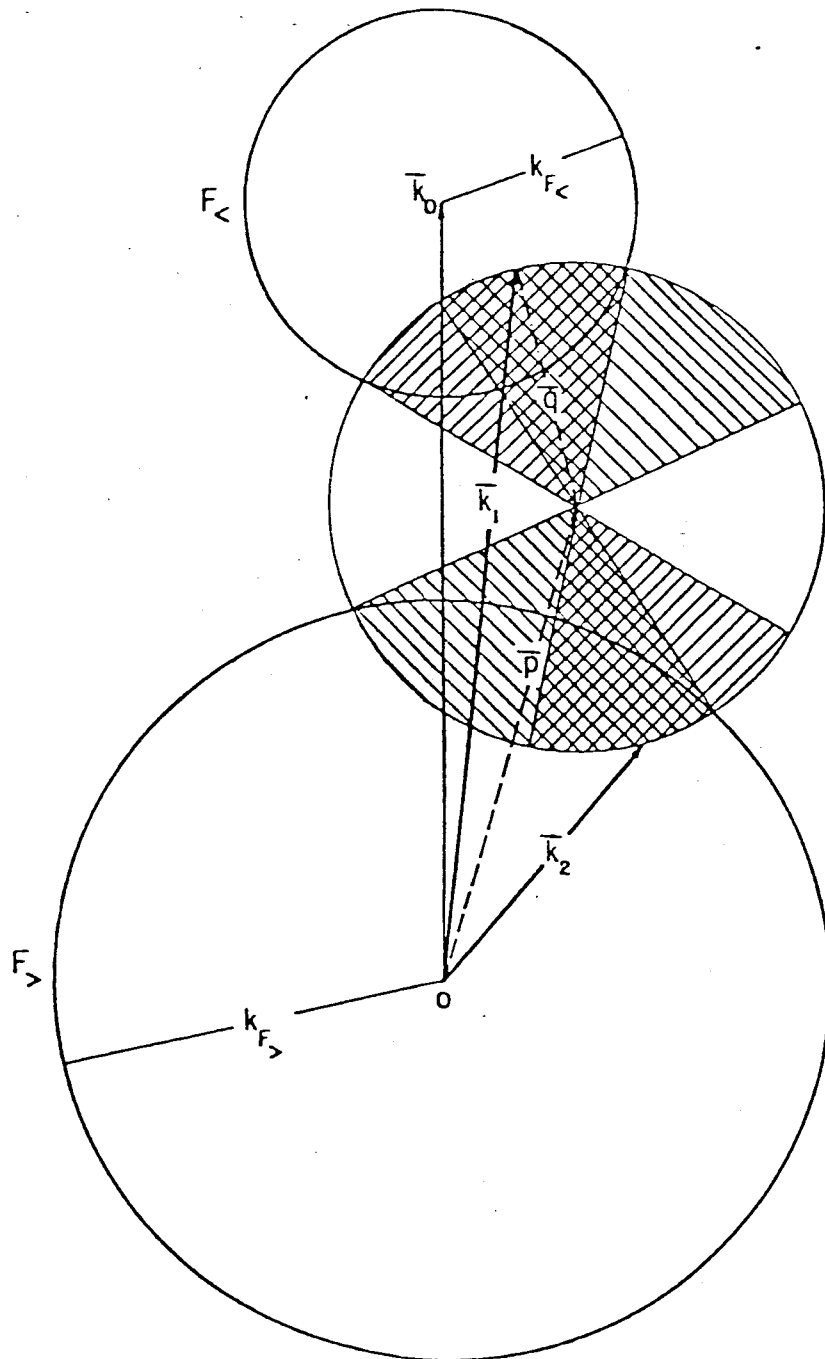


FIGURE A.1